Changes in Surface Air Temperature Caused by Desiccation of the Aral Sea

ERIC E. SMALL

Department of Earth and Environmental Science, New Mexico Institute of Mining and Technology, Socorro, New Mexico

LISA CIRBUS SLOAN

Department of Earth Science, University of California, Santa Cruz, Santa Cruz, California

DOUG NYCHKA

Climate and Global Dynamics Division, National Center for Atmospheric Research, Boulder, Colorado*

(Manuscript received 23 August 1999, in final form 8 February 2000)

ABSTRACT

A statistical method for establishing the cause–effect relationship between a land surface modification and some component of observed climatic change is presented. This method aids attribution in two ways. First, the climatic changes that are unique to the area influenced by some land surface modification are identified. This isolates changes caused by the spatially restricted forcing from changes caused by other factors. Second, most of the short-term climatic variability in the records from the affected area is removed based on information from the surrounding region. This makes it possible to identify smaller climatic changes. This method is used to identify the changes in surface air temperature that have resulted from desiccation of the Aral Sea (1960–97). Desiccation has weakened the ''lake effect'' of the Aral Sea, so regional climatic changes are expected.

Substantial temperature trends, unrelated to desiccation, are observed across a broad region of central Asia (~2000 km) between 1960 and 1997. These trends are similar in magnitude to the changes from desiccation. These trends are removed from the records from the Aral region because they would enhance or offset the local temperature changes caused by desiccation. There is also substantial year-to-year temperature variability that is spatially coherent across central Asia. The method used here removes ~80%–90% of this short-term variability in the observed temperature records from the Aral region. This lowers the climate change detection limit from ~3°–8°C to ~1°–2°C, which improves the identification of the spatial extent of the desiccation-induced changes.

The climate records from around the Aral Sea show dramatic temperature changes between 1960 and 1997, once regionally coherent trends and variability are removed. Mean, maximum, and minimum temperature near the Aral Sea have changed by up to 6°C. Warming (cooling) is observed during spring and summer (autumn and winter), as expected to accompany the diminished lake effect caused by desiccation. The magnitude of temperature changes decreases with increasing distance from the 1960 shoreline, with changes extending up to ~200 km from the shoreline in the downwind direction. An increase in diurnal temperature range of 2°–3°C is observed in all months, demonstrating a weakening of the lake's damping effect on the diurnal temperature cycle.

1. Introduction

In order to understand why climate changes through time, it is critical to establish cause–effect relationships between certain forcings of the climate system, both anthropogenic and natural, and different components of observed climatic changes. Local or regional climate may change as a result of spatially restricted anthropogenic modifications of the land surface, including deforestation, irrigation, urbanization, and desiccation of inland water bodies. Establishing the climatic response to regional and local changes of the land surface is important for several reasons. First, this enables us to better understand how human modifications of the environment influence climate (e.g., Chase et al. 1999). Second, it reveals the processes that govern land–atmosphere interactions (Shuttleworth 1991). Third, a substantial fraction of global climate change may reflect changes driven by regional-scale forcings (Schneider 1994). And fourth, land surface modification, such as urbanization, may introduce biases into the observational networks used to study global change (Karl et al. 1988). In this paper, we will describe a statistical

* The National Center for Atmospheric Research is sponsored by the National Science Foundation.

Corresponding author address: Eric Small, Department of Earth and Environmental Science, New Mexico Tech, Socorro, NM 87801. E-mail: esmall@nmt.edu

method appropriate for identifying the climatic changes driven by local to regional land surface modifications. Then we will use this method to examine the climatic response to anthropogenic desiccation of the Aral Sea between 1960 and 1997.

Establishing a cause–effect relationship between some forcing and an observed climatic change is difficult for several reasons. First, numerous forcings influence the climate system simultaneously (Schneider 1994). The effects of these forcing may be opposite in sign, persist over timescales that differ by several orders of magnitude, and act on different spatial scales. Therefore, establishing the climatic response to a particular forcing requires that the climatic changes due to the forcing in question are isolated from all other changes, as well as from internal climate system variability (Hurrell and van Loon 1997). The second reason that attribution is difficult is that the magnitude and nature of the forcing is typically poorly constrained. For example, estimates of the magnitude of deforestation over West Africa vary considerably (e.g., Gornitz 1985; Myers 1991). Third, variability of the climate system hinders attribution by obfuscating the signal in the observed record (Zheng et al. 1997), even if the climatic change is shown to be outside of the range of natural variability. And finally, short climate records, missing data, and station inhomogeneities further hinder accurate trend detection.

One method for assessing the effects of land surface modifications is to use a physically based model (e.g., Small et al. 2001, this issue). A complementary method is to examine climate records using a statistical model. One problematic statistical approach is to compare mean climatic conditions from disturbed and undisturbed locations and attribute the differences between them to the modification of the land surface. For example, Barnston and Schickedanz (1984) reported that irrigation lowered maximum temperature by $\sim$2°C in the southern Great Plains, based on a comparison of temperature in adjacent irrigated and unirrigated areas. However, all or part of the observed temperature difference could be the result of constrasts in the local landscape (elevation, soil, etc.) or background climate (Lowry 1977) unrelated to irrigation. Another problematic approach is to identify climatic changes through time at some location and attribute the changes to concomitant land surface changes. For example, changes in air temperature, near-surface wind, and precipitation have accompanied, and been attributed to, irrigation in southern Israel (Otterman et al. 1990; Ben Gai et al. 1993; Alpert and Mandel 1986). However, some component of these observed trends may be caused by changes in synoptic climate rather than irrigation (Steinberger and Gazit-Yaari 1996). These problems can be minimized by combining the two different approaches—temporal changes in the difference between disturbed and undisturbed locations are attributed to concomitant land surface changes (Lowry 1977). This sort of approach has been used to assess the effects of irrigation (e.g., Fowler and Helvey 1974) and urbanization (e.g., Karl et al. 1988). We use an extension of this approach to examine the effects of Aral Sea desiccation.

The surface area of the Aral Sea was $\sim$65 000 km^2 in 1960, making it the fourth largest inland water body on Earth (Fig. 1). The Aral Sea is a terminal lake (no outflow) and only receives inflow from the Amu and Syr Darya Rivers. After 1960, agricultural diversions of river water increased substantially throughout the Aral Sea drainage basin (Micklin 1988). The river inflow to the Aral was greatly reduced because most of the diverted water was lost to evapotranspiration and groundwater recharge. As a result of the reduced inflow, the water balance of the Aral Sea became negative after 1960—evaporation from the lake surface was greater than the sum of on-lake precipitation and the reduced stream flow. The result was 1) a $\sim$60% decrease in lake surface area, 2) a decrease in mean depth from 15 to 8 m, 3) a 80% decrease in volume, and 4) an increase in salinity from 10 to $>$35 ppt.

Desiccation, therefore, has resulted in a substantial and spatially extensive modification of the land surface that should impact regional climate. Roughly 40 000 km^2 that was once part of the lake is now sparsely vegetated sand and evaporite deposits, leading to important changes in the thermal, moisture, and radiative properties of the land surface. The $\sim$25 000 km^2 of the Aral Sea that remains has also been affected. The lake's thermal capacity has decreased due to the reduction in water depth, leading to an increase (decrease) in lake surface temperature and evaporation rate during the spring and summer (autumn and winter) (Small et al. 2001). Previous observational (Chagnon and Jones 1972) and modeling studies (e.g., Bates et al. 1995; Hostetler et al. 1994) have shown that lakes similar in size to the Aral Sea, such as the Great Lakes or paleolake Bonneville, influence climate over a distance of several hundred kilometers. This ''lake effect'' is primarily driven by the seasonally varying water-to-land temperature contrast (Miner and Fritsch 1997). Seasonal variations of lake surface temperature lag behind those of land surface temperature because more heat is stored in the lake. Desiccation has weakened the lake effect caused by the Aral Sea. The expected outcome is warmer (cooler) air temperatures around the lake in spring and summer (autumn and winter) and an increase in diurnal temperature range in all seasons.

The following climatic changes have been observed in the Aral region and have been attributed to desiccation: 1) changes in air temperature, including a shortening of the growing season (Smith 1994); 2) decreased relative humidity; and 3) more severe ''droughtiness'' (Dukhovnyi et al. 1984). These changes were based on short records (20 yr) from one or two stations and were not evaluated in terms of statistical significance. In addition, no effort was made to determine if these changes were unique to the Aral region, or were instead observed

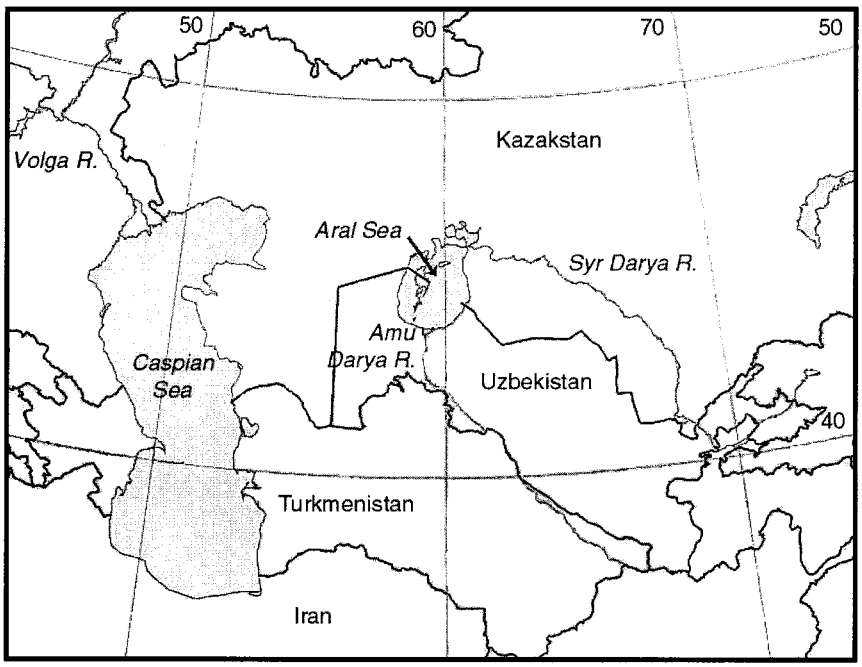

FIG. 1. Map of Aral Sea region. Shaded areas show Aral and Caspian Seas. Numbers represent degrees of longitude and latitude.

across a more extensive region and therefore unrelated to desiccation.

This paper has two major parts. First, we describe and evaluate a method to identify the climatic changes resulting from a spatially restricted modification of the land surface. This method aids attribution in two ways. First, the climatic changes caused by the spatially restricted forcing are isolated from changes caused by various other factors. This is accomplished by identifying the climatic changes that are unique to the area influenced by the land surface modification. Second, most of the ''noise'' in the climate records from the affected area is removed based on information about short-term variability from the surrounding region. This makes it possible to identify and attribute smaller climatic changes.

Second, we use this method to investigate how desiccation of the Aral Sea has influenced air temperature in the surrounding region. We examine changes in surface air temperature at the monthly timescale, including changes of the mean, extremes, and the diurnal temperature range (DTR). We focus on changes in temperature because data for other climate variables is relatively limited in the Aral Sea region. The following questions will be addressed. 1) How does the magnitude of temperature changes vary spatially around the Aral Sea? 2) How do the observed changes vary throughout the year? 3) How do the changes driven by desiccation compare to broader-scale climatic changes and variability over the same interval? Answers to these questions will allow us to assess how a human disturbance of the hydrological system (diversion of streamflow) in central Asia has affected regional climate. In addition, this information will provide a more complete understanding of how large lakes influence regional climate, which has implications for both paleoclimate (e.g., Sloan 1994) and present-day hydrologic studies (e.g., Lofgren 1997).

The plan of this paper is as follows. We first describe the air temperature data used in this analysis (section 2). Then we describe the approach used to identify the changes in air temperature driven by Aral Sea desiccation (section 3). Our results are described in section 4. A discussion of our results (section 5) and conclusions (section 6) follow.

2. Observations

We used surface air temperature observations from the Global Summary of Day Data (GSDD), available from the National Climatic Data Center (NCDC). This dataset is derived from the synoptic/hourly observations in the Air Weather Series DATSAV2 surface dataset. We chose to use the GSDD because it includes records from numerous stations in the Aral Sea region (Fig. 2). Other datasets, such as the Global Historical Climatology Network (GHCN), may include more refined data than those used here. However, the station density in these datasets is insufficient for studying local climatic changes in the Aral region. For example, there are only three stations within 500 km of the Aral in the GHCN, compared to ~50 in the GSDD. Overall, we used GSDD observations from more than 170 stations in central Asia (Fig. 2) covering the period of Aral desiccation (1960–

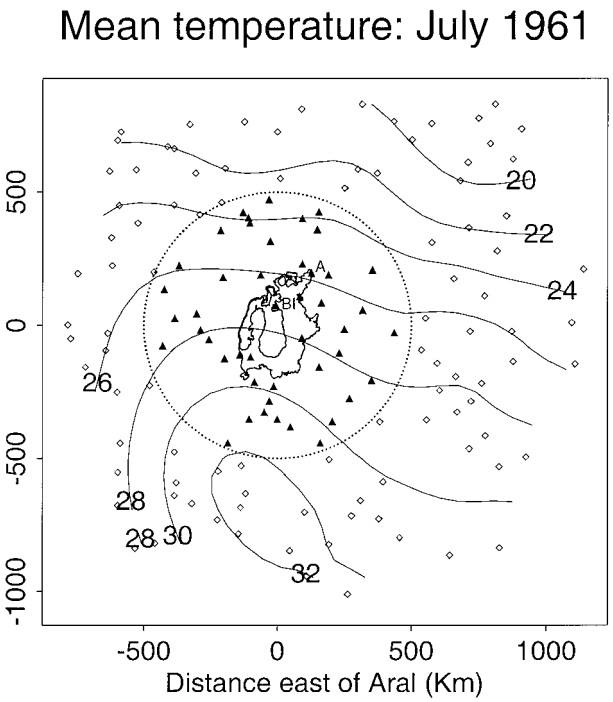

FIG. 2. Region of central Asia examined in this study. The axes show distance from the center of the Aral Sea (60°E, 45°N; km). The 1960 and 1999 shorelines of the Aral Sea are shown. The dotted line represents the boundary of the analysis region. Stations used to estimate regional (open diamonds) and local temperature anomalies (filled triangles) are plotted. The contour lines show the regional mean temperature field for Jul 1961 (°C), interpolated from observations outside of the analysis region. Here ''A'' is the station Aral'sk and ''BI'' is the station Barsakelmes Island.

97). Temperature observations from the predesiccation interval were not examined because few data exist prior to 1960. In addition, we did not evaluate changes in precipitation throughout the desiccation interval because precipitation records from many stations in central Asia are incomplete (Small et al. 1999).

We used daily values of mean, maximum, and minimum temperature from the GSDD. In addition, we calculated the DTR for all days when both maximum and minimum temperature were reported. The daily mean temperature values in this dataset are the average of typically eight synoptic observations (i.e., observations every 3 h), not the average of the daily maximum and minimum temperature. Maximum and minimum temperature are most frequently taken from explicit extreme temperature observations. However, the maximum or minimum of the synoptic observations was used when the explicit measurements were missing but all synoptic observations were available.

We calculated monthly mean values of all four temperature variables from the daily data. When daily values were not available for each day of a month, the monthly mean was determined from the available data. The number of missing daily values in each month was recorded and used to weight the monthly means in each step or our analysis (described below).

There are two problems with the GSDD data. First, the data from NCDC have not been adjusted for inhomogeneities (Karl and Williams 1987). Therefore, changes in observation method, stations moves, and other factors may introduce errors into the data. Second, some of the stations do not have continuous records from 1960 to present. For example, the records from several stations in Uzbekistan begin around ~1970. Our results demonstrate that these data quality issues introduce only minor errors into our analysis, as compared with the substantial climatic changes that have occurred in the Aral Sea region between 1960 and 1997 (section 5b).

3. Methods

a. Problem of isolating a local climatic change

We now describe the challenge of identifying the climatic change resulting from a spatially restricted forcing such as desiccation of the Aral Sea, using a hypothetical temperature record from a station on the sea's shoreline. We expect that July (January) mean air temperature would increase (decrease) along the shoreline as a result of desiccation. This warming would be easily identifiable if desiccation were the only forcing of the climate system and there were no temporal variability of temperature (Fig. 3a).

Of course, air temperature throughout central Asia varies through time. This introduces changes into the shoreline record that are unrelated to desiccation. The type of problem introduced by temperature variations that are spatially coherent across a broad area depends on the timescale of the variations. First, changes that are in a consistent direction throughout the desiccation interval (~40 yr) could enhance or offset the local warming from desiccation. Global forcings of the climate system (e.g., enhanced greenhouse gases) or long-term climatic variability would have this effect. It is not possible to distinguish between the changes caused by desiccation and the changes common to a broad region using only a single temperature record. Second, regionally coherent variability on timescales shorter than the desiccation interval introduce noise into the record (Fig. 3c) that makes identifying local climatic changes more difficult (section 3e).

The hypothetical record from the shoreline station reflects the sum of the temperature anomalies from the three components described above (Fig. 3d). The warming caused by desiccation would be overestimated if we were to use the observed record to gauge the effects of desiccation. In addition, the change would be poorly constrained if the noise in the record was not reduced. This example demonstrates that the observed record of temperature anomalies, $O(t)$, at some station can be modeled as follows:

$$O(t) = R_T(t) + R_v(t) + L(t) + \varepsilon, \qquad (1)$$

where $R_T(t)$ represents anomalies from spatially coherent trends that are of a consistent sign over the time period examined (Fig. 3b), $R_v(t)$ represents anomalies from short-term variability that is spatially continuous (Fig. 3c), $L(t)$ are local anomalies unique to some specified area (Fig. 3a), and ε is noise in the record due to incomplete sampling throughout a month, changes in observing practices, or variability that is not spatially continuous.

b. Approach of isolating the local climate change

Our goal is to identify the climatic changes that are caused by some spatially limited alteration of the land surface. To accomplish this goal, we must identify the component of climatic changes in the observed record $O(t)$ that are unique to the area influenced by the local forcing. Presumably, these local anomalies $L(t)$ are the result of the local land surface modification being studied. However, the influence of other forcings in the modified area may also be important and needs to be assessed. In order to isolate the local signal, we remove any anomalies related to regionally consistent temperature trends, $R_T(t)$, and variability, $R_v(t)$, from the observed record of temperature anomalies:

$$L(t) + \varepsilon = O(t) - [R_T(t) + R_v(t)]. \qquad (2)$$

In the context of the previous example, we isolate the warming caused by desiccation (Fig. 3a) from the observed record (Fig. 3d) by subtracting off the regionally coherent warming and variability (Figs. 3b and 3c). In the preceding example, we separated regional temperature trends and variability because they hinder the identification of local climatic changes in different ways. However, it is the sum of regionally consistent temperature trends and variability, $R(t) = [R_T(t) + R_v(t)]$, that we actually removed from the observed record.

We identify the sum of regionally coherent trends and variability, $R(t)$, by using temperature observations from stations outside of the area influenced by Aral desiccation (Fig. 2). This requires identifying an ''analysis region'' that includes the entire area affected by desiccation [i.e., $L(t) = 0$ outside of this area]. Model results suggest that the climatic effects of desiccation do not extend beyond 500 km from the center of the Aral Sea (Small et al. 2001). Therefore, we define the outer boundary of the analysis region to be a circle with a radius of 500 km centered on the sea (Fig. 2). We cannot be certain a priori that the climatic effects of desiccation do not extend beyond this boundary (Lowry 1977). However, it is possible to test if this is the case. Below, we show that the analysis region used here is sufficiently large (section 4e).

We make two assumptions when we use data from outside of the analysis region to identify the component of the observed temperature variations near the Aral Sea that is due to the combinations of regionally coherent trends and variability. First, we assume that the climatic changes caused by desiccation do not extend beyond the boundary of the analysis region. If this assumption is incorrect, than the regional signal will include changes from desiccation, and the magnitude of the local changes from desiccation will be underestimated. Because the climatic effects of desiccation should decrease with distance from the shoreline (Small et al. 2001), this assumption is a better approximation the larger the radius of the analysis region is. The second assumption is that both regional climatic trends and variability are spatially continuous at a length scale as large as or larger than the analysis region. If this assumption is correct, then

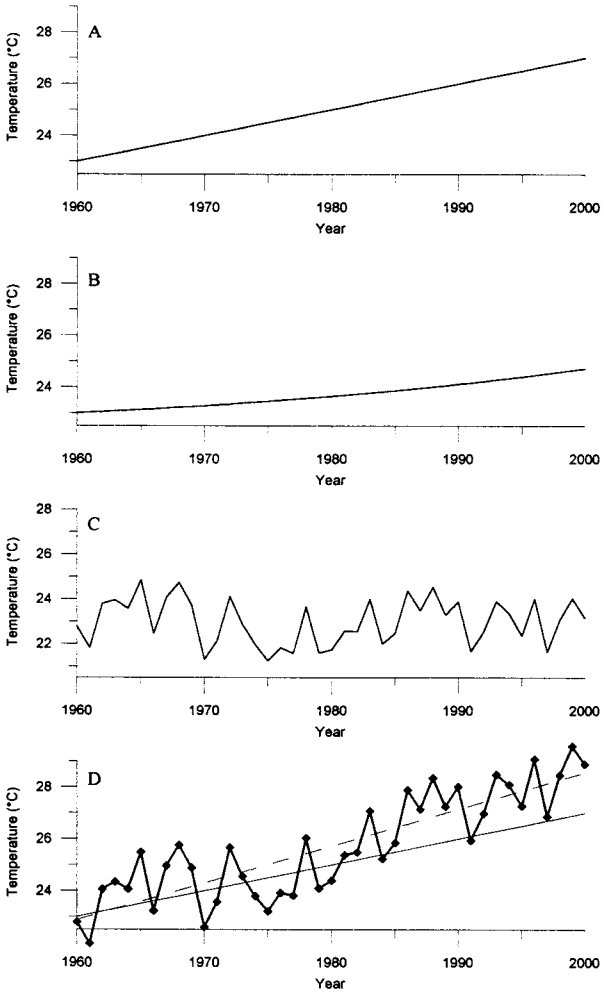

FIG. 3. Hypothetical example of the different components of the mean temperature record for Jul from a station on the Aral Sea shoreline. (a) Local temperature change caused by desiccation, $L(t)$; (b) temperature changes across central Asia that are consistent in sign throughout the 40-yr interval, $R_T(t)$; (c) short-term temperature variability across central Asia, $R_v(t)$; (d) the observed record, $O(t)$, which is the sum of the anomalies from (a)–(c) (thick line with points). A linear fit to the observed time series (dashed line) and the local temperature change from Aral desiccation (thin solid line) are also included in (d).

observations from outside of the analysis region can be used to quantify regional trends and variability within the area influenced by Aral desiccation. Obviously, this assumption is more accurate for a smaller analysis region. The optimal analysis region, therefore, represents a tradeoff between these two assumptions. A larger area ensures that the local and regional changes are separated but reduces the correlation between ''regional'' trends or variability [$R_T(t)$ or $R_v(t)$] in the analysis region and the surrounding areas. Below, we show that these two assumptions are good approximations for the analysis region (500-km radius) used here.

c. Steps taken to isolate changes

We take the following steps to isolate the climatic change unique to the Aral region. First, we construct a regional temperature field for central Asia based only on temperature observations from outside the boundary of the analysis region (Fig. 2). This is done independently for each month of each year (e.g., July 1961) throughout the desiccation interval (1960–97) and for each temperature variable (mean, maximum, minimum, and DTR). Data from ~120 stations within ~500 km of the analysis region are interpolated using a thin plate spline (TPS) analysis (Nychka and Saltzman 1998). Temperatures are not adjusted for differences in elevation because the elevation of all stations used here is within ~200 m of Aral Sea level. Each value used in the TPS interpolation is weighted by the number of temperature observations contributing to the monthly mean. An interpolation scheme such as TPS is required for our analysis because the temperature distribution across central Asia is not zonally symmetric (Fig. 2).

For each temperature variable and month, the interpolated temperature fields from 1960–97 are used to determine the regional temperature time series at each observation station within the analysis region. This time series is converted to regional anomalies, $R(t)$, by subtracting the spatially varying long-term mean (1960–97). Here $R(t)$ is different for each station because the interpolated temperature fields vary in space across the analysis region (Fig. 2). The time series of local anomalies at each station is calculated by subtracting the time series of regional anomalies estimated for that station from the observed temperature anomaly record, $L(t) = O(t) - R(t)$. The preceding steps yield three time series of temperature anomalies for each station in the analysis region: observed, regional, and local (Fig. 4).

Last, we calculate linear trends from the time series of observed, regional, and local temperature anomalies using a least squares method. For the observed and local records, the number of observations that contribute to each monthly mean are used as weights in the regression. This weighting is not completed for the regional time series because each TPS field is constructed from a series of monthly means calculated from a variable number of observations. Each trend is converted to a temperature change over the desiccation interval by multiplying the trend (°C yr^{-1}) by the number of years ($n = 38$; 1960–97). Several stations have records that begin around 1970. For these stations, the temperature changes are only calculated over the period of record, which provides a minimum estimate of temperature changes throughout the desiccation interval.

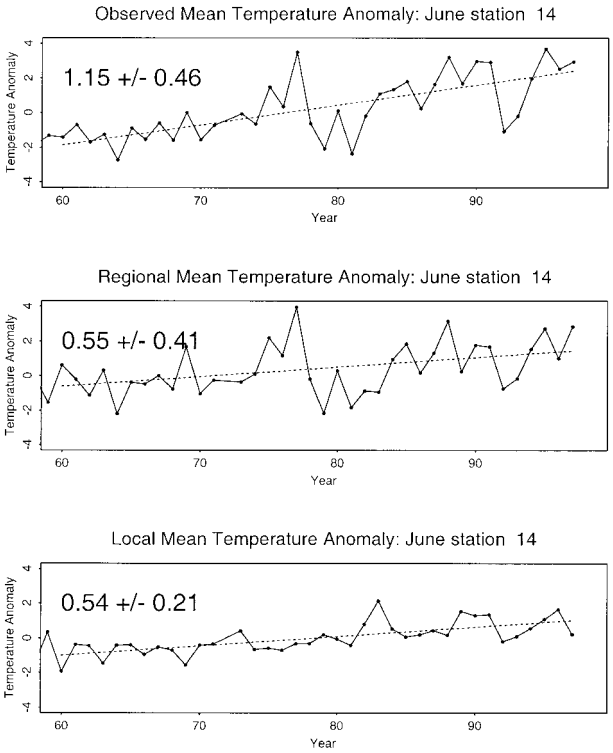

FIG. 4. Jun mean temperature anomalies (solid lines; °C) from 1960 to 1997 from Aral'sk (station ''A'' in Fig. 2): (top) observed temperature anomalies, $O(t)$; (middle) regional temperature anomalies, $R(t) = [R_T(t) + R_v(t)]$; and (bottom) local temperature anomalies, $L(t)$. The dashed line is a linear fit to the data. The slope and 95% confidence interval estimate on the slope are also shown (°C decade^{-1}).

Many of the station records used to construct the regional temperature fields are not continuous between 1960 and 1997. Discontinuous records can introduce errors into gridded datasets if the temperatures at stations with discontinuous data are anomolously warmer or cooler than neighboring values (Peterson et al. 1998). We examined the influence of discontinuous records on our spatial interpolation by recalculating the regional time series, $R(t)$, for July mean temperature using the First Difference Method (FDM) of Peterson et al. (1998). The FDM approach yields the year-to-year temperature differences at each station. These differences, instead of the observed temperatures, were then interpolated across the analysis region as described above. At each station within the analysis region, the FDM regional time series is nearly identical to the regional time series generated using the observed temperatures. Therefore, the time series of local temperature anom-

alies calculated using the two methods are also nearly identical. This test demonstrates that interpolating observed temperatures from discontinuous records introduces negligible errors into our analysis.

d. Examples of the analysis

The June mean temperature record from Aral'sk, a city located on the northeastern 1960 shoreline of the Aral (Fig. 2), demonstrate the important features of this analysis: 1) regionally coherent trends must be removed to identify local climatic changes; and 2) reducing the noise in observed records facilitates trend detection. The observed temperature record shows a warming of 1.15° ± 0.46°C decade^{-1} over the past 40 yr (95% confidence interval estimate of linear trend; Fig. 4a). This change is reasonable as warming is expected to accompany desiccation during summer. However, the regional anomalies show June mean temperatures have increased across central Asia, so the warming at Aral'sk is probably not the result of desiccation alone. At Aral'sk, the regional warming (Fig. 4b) is roughly half of that in the observed record (Fig. 4a). The time series of local temperature anomalies indicates a local warming of only 0.54° ± 0.21°C decade^{-1} (Fig. 4c). This shows that only half of the change observed at Aral'sk is actually caused by desiccation.

The year-to-year temperature fluctuations observed at Aral'sk (Fig. 4a) are similar to the fluctuations in the regional time series (Fig. 4b), which depict interannual variability outside of the analysis region. This qualitatively demonstrates that a large component of interannual variability in central Asia is coherent at the length scale of the analysis region. Otherwise, year-to-year fluctuations within (Fig. 4a) and outside (Fig. 4b) of the analysis region would not be correlated. We present a more quantitative assessment or regional coherence in section 3e. Because the interannual variability is spatially continuous, most of the noise in the observed record (Fig. 4a) is absent from the local time series (Fig. 4c). This lowers the magnitude of the confidence interval estimate of the local climatic change by half.

Regional climatic changes may be opposite in sign from local changes, which offsets the local signal rather than enhancing it. For example, the observed temperature record from Barsakelmes Island (BI in Fig. 2) shows that mean temperature in January has increased since 1960 (not shown). This warming is unexpected because desiccation should result in cooler air temperatures during winter. The regional anomalies at Barsakelmes Island exhibit a greater warming trend than the observed anomalies. So, once the regional anomalies are removed from the observed time series, the record of local anomalies shows the cooling that is expected to accompany desiccation. This example demonstrates how ignoring regionally coherent trends may yield local climatic changes that are of the wrong sign.

e. Removing noise from temperature records

The record from Aral'sk (Fig. 4) shows that most of the year-to-year variability in the observed time series is regionally coherent. Removing this variability is particularly important when the magnitude of the trend is small compared to the variability. When this is the case, noise in the record may raise the confidence interval estimate so much that detection of a trend is not possible even though one exists—one cannot disprove the null hypothesis that the trend is zero. We now show that the climate change detection limit (i.e., the minimum change that can be identified) for the observed records is much greater than for the local time series.

The minimum trend that can be detected from a time series of length n, in terms of the slope b, is

$$|b| > t(\alpha/2, \mathrm{df}_{n-2})S_b, \tag{3}$$

where t is the critical t value for some significance level (α) and degrees of freedom (df), and S_b is the standard error of the slope. The degrees of freedom is the number of years in the temperature records. The standard error of the slope is

$$s_b^2 = \frac{s_e^2}{\sum x^2 - \left[\left(\sum x\right)^2 \Big/ n\right]}. \tag{4}$$

The denominator is the sum of the squares of the independent variable (time) and the numerator s_e^2 is the variance of the residuals or errors about the regression line:

$$s_e^2 = \frac{\sum (y - \hat{y})^2}{n - 2}, \tag{5}$$

where $\hat{y}$ is the predicted temperature value from the regression equation. Differences in the detection limit, from station to station or between months or variables, arise from differences in the variability about the regression line (s_e^2). This variability reflects year-to-year climate fluctuations if there is no misfit to the data (i.e., a linear fit is appropriate). Therefore, the climate change detection limit is higher for the observed records because they include more substantial short-term variability.

The detection limit for the observed temperature records [$O(t)$], excluding DTR, is typically greater than 3°C and varies substantially from month to month (Fig. 5). For example, the median detection limit for observed mean temperature is 8°C during January and is only 3°C during July. The difference reflects the greater interannual temperature variability observed during the winter season. The detection limit for DTR is much lower than for mean, maximum, and minimum temperatures because the interannual variability in this parameter is much less. The detection limit is much higher for some stations than for others, as shown by the vertical extent of the box and whiskers in Fig. 5. The stations with the most complete records have the lowest detection limits,

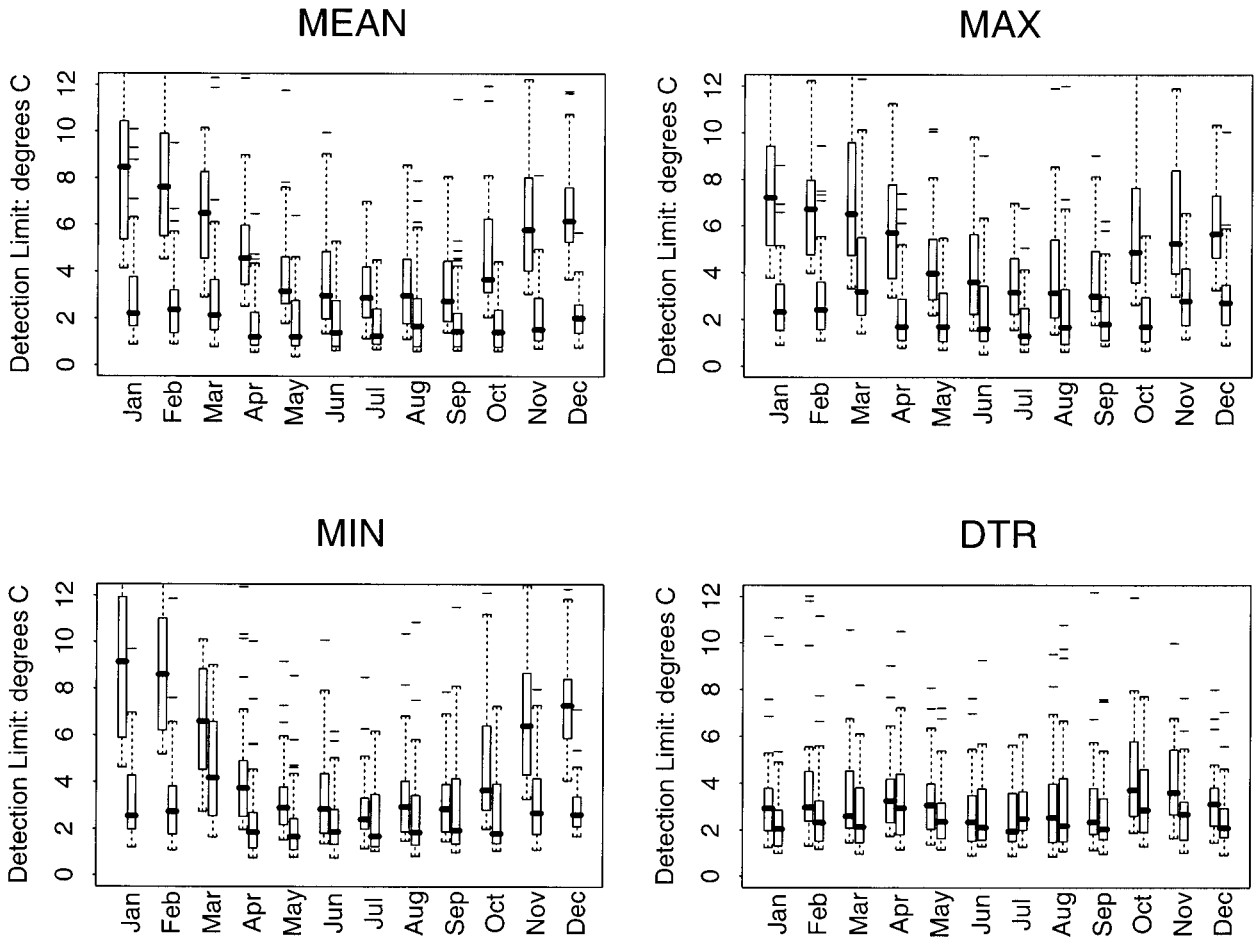

FIG. 5. Box and whisker diagrams of the climate change detection limit for all stations in the analyzed region, for each temperature variable examined. There are two box and whiskers for each month: the left shows the detection limit for the observed time series and the right the limit for the local time series. The solid horizontal bar shows the median detection limit. The vertical extent of the box represents the range of the middle half of the data (from 25% to 75%). The whiskers extend to 1.5 times the interquartile range. The isolated horizontal bars denote outliers.

suggesting that the ''error'' component in Eq. (2) hinders trend detection at some stations. The detection limits from the observed records are greater than the temperature changes expected to accompany a variety of land surface changes, particularly toward the margin of the region influenced by the change.

The detection limits in the local time series [$L(t)$] are greatly reduced in comparison with those for the observed records—the median detection limit is ~1°–2°C in all months and for all variables (Fig. 5). This shows that much smaller changes can be detected in the local time series because the noise that reflects regionally coherent short-term climate variability has been removed. The percentage of variance about the regression line (s_e^2) or noise removed from the observed records is greater than 90% during winter and is ~80% or lower in the summer (Fig. 6). The variance reduction is minimal for DTR and during some summer months because there is little variability in the observed records in these cases.

The reduction of variance and detection limit in the local time series shows that the second assumption described above is accurate—short-term temperature variations from the area surrounding the analysis region, $R_v(t)$, accurately portray short-term variations inside the region. If variability was not spatially coherent at the length scale of the analysis region, subtracting regional anomalies would not substantially decrease the variance around the regression lines in the local times series. Based on this result, it seems reasonable that longer-term temperature trends $R_T(t)$ are also correlated at the length scale of the analysis region.

4. Local changes in air temperature

a. Mean temperature

We have used the method described in section 3 to identify temperature trends unique to the Aral Sea region between 1960 and 1997. Very few of the observed

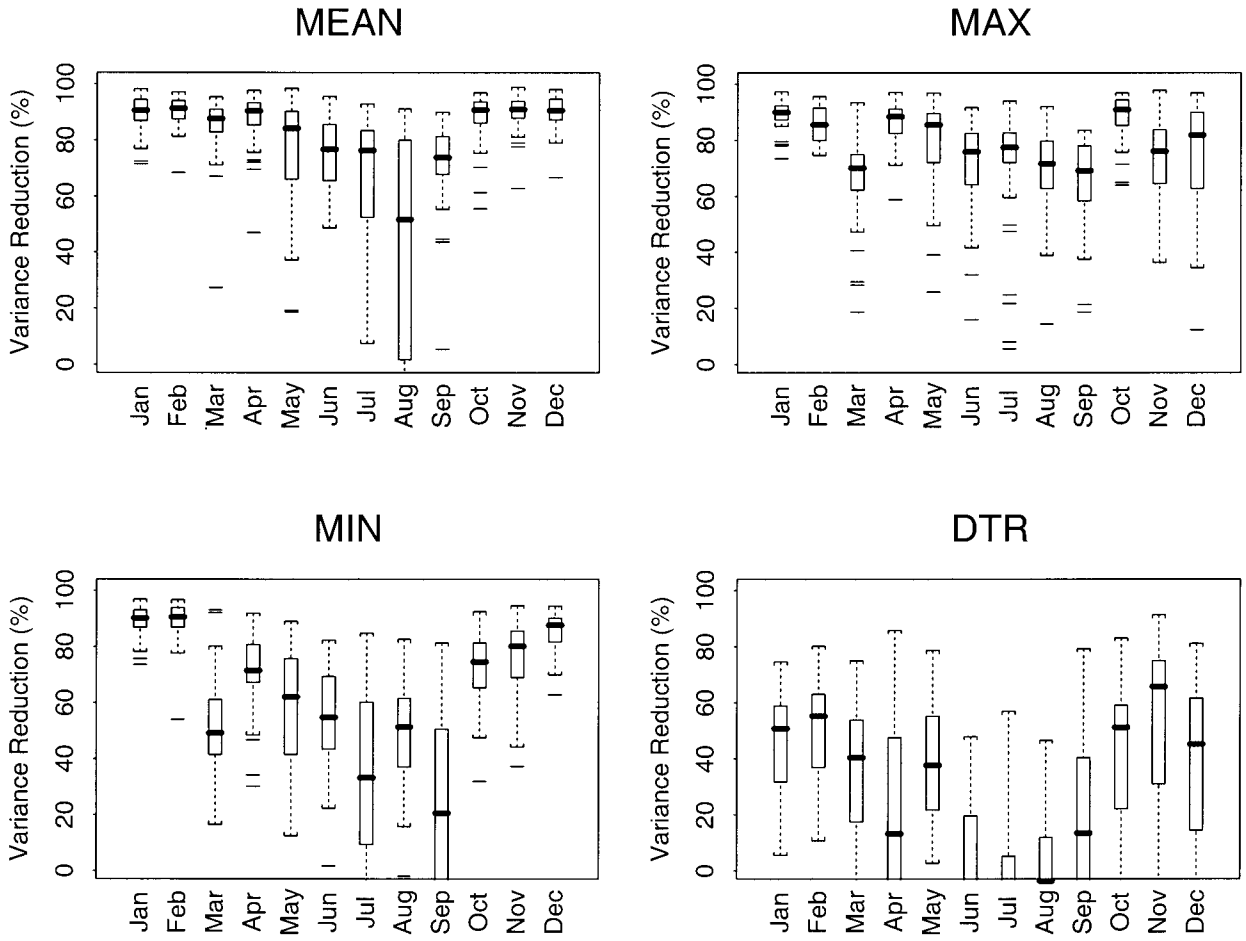

FIG. 6. Box and whisker diagrams of the percent of variance about the regression line in the observed records that is removed when constructing the local time series, for all stations in the analyzed region. Box and whiskers show the same statistical features as in Fig. 5.

time series, $O(t)$, exhibit statistically significant trends in mean temperature (Table 1). This is expected given the high detection limit of the observed records (Fig. 5). For example, few stations exhibit statistically significant changes in May (Fig. 7a), a month when the effects of desiccation should be substantial. There are many more significant trends in the time series of local temperature anomalies $L(t)$, as shown by maps of observed and local mean temperature change in May (Figs. 7a and 7b, Table 1). Again, this demonstrates that removing regionally coherent variability [$R_v(t)$] aids the identification of local climatic changes.

The changes in local temperature anomalies $L(t)$ along the shoreline of the Aral Sea are very large. Changes in mean temperature of 4°C (1.0°C decade^{-1}) or greater are common (Fig. 7). The local changes are greatest in magnitude near the Aral Sea and diminish with increasing distance from the shoreline (Figs. 7 and 8). Larger changes exceed the detection limit at higher-confidence levels [Eq. (3)]. Therefore, the most significant changes (>99% confidence level) are clustered around the Aral Sea and there are few or no significant changes far from the shoreline (Fig. 7). The pattern of intense changes around the sea and minimal changes elsewhere demonstrates that we have identified a local climatic change that is spatially correlated with the Aral Sea. In addition, this pattern is consistent with the assumption that the climatic changes isolated within the analysis region do not extend into the surrounding region. This assumption is evaluated in more detail below (section 4e).

Local temperature changes are observed further from the shoreline in the downwind direction than on the upwind side (Fig. 7). This pattern provides additional evidence that the local changes are spatially linked to the Aral Sea. During July, the mean local temperature

TABLE 1. Percent of station–month combinations in the analysis region with temperature trends over the period 1960–97 that are significant at the 95% confidence level, for the observed and local time series.

	Mean	Maximum	Minimum	DTR
Observed	5	10	10	19
Local	19	18	19	19

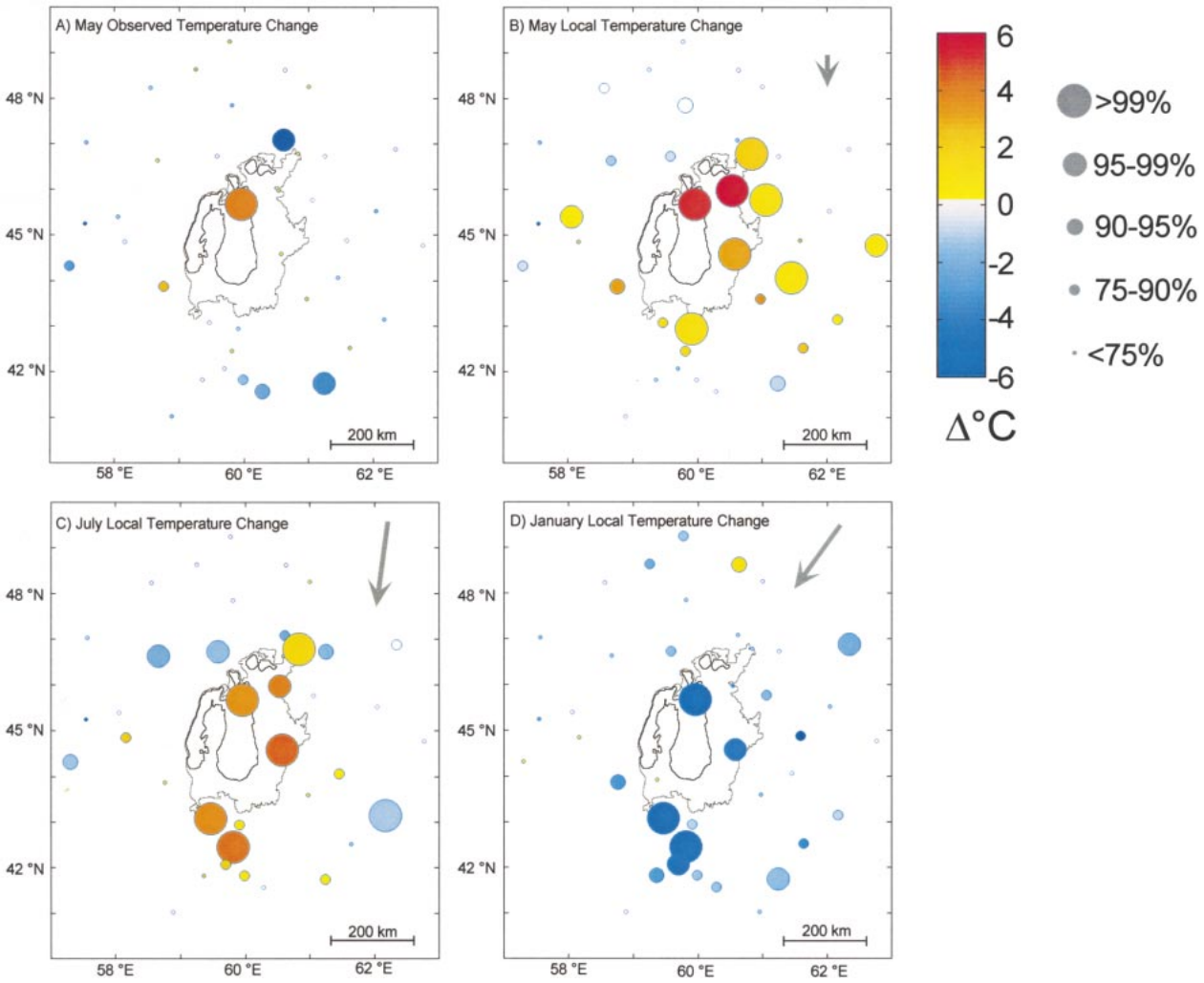

FIG. 7. Maps of mean temperature change for the analysis region: (a) observed changes in May; (b) local changes in May; (c) local changes in Jul; and (d) local changes in Jan. The circles are placed at the location of meteorological stations. Circle color denotes the temperature change (°C) based on linear trend analysis (color bar at top right). The size of the circles represents the probability that the detected changes are significant (key at top right). The 1960 (light gray) and 1999 (dark gray) Aral Sea shorelines are shown. Gray arrow shows prevailing *surface* wind direction in each month. Winds aloft are from the west in Jan and May and from the north in Jul. The relative length of wind arrows qualitatively shows average wind speed.

changes extend farthest to the south of the Aral Sea. The prevailing surface winds, as well as winds aloft, are consistently from the north during this month (Fig. 7c) (Lydolph 1977). The prevailing surface winds are from the northeast during January (Lydolph 1977). Again, the local temperature changes are most concentrated on the downwind side (Fig. 7d). Local changes are observed in all directions but to the north of the sea during May. During this month, the surface winds are relatively variable but typically have a northerly component.

The sign of the local temperature changes in the Aral Sea region varies seasonally. In general, warming predominates between April and July, cooling predominates between September and January, and changes in other months are relatively minor. These seasonal variations are apparent in the maps of July and January local change (Figs. 7c and 7d) or in the annual cycle of local changes at a single station (Fig. 9). For example, the maximum warming at Barsakelmes Island (5°C) occurs during May and the maximum cooling (7°C) occurs during January, representing an increase in the annual mean temperature range of ~12°C (Fig. 9a). The annual cycle of temperature changes is similar at other stations, except that the magnitude of the changes decreases rapidly with distance from the shoreline (Fig. 9b). The seasonal variations of local temperature trends are consistent with the changes expected to accompany desiccation. The Aral Sea is cooler (warmer) than the adjacent land during spring and summer (autumn and winter) and therefore has a cooling (warming) effect during this season. The magnitude of the thermal lake effect

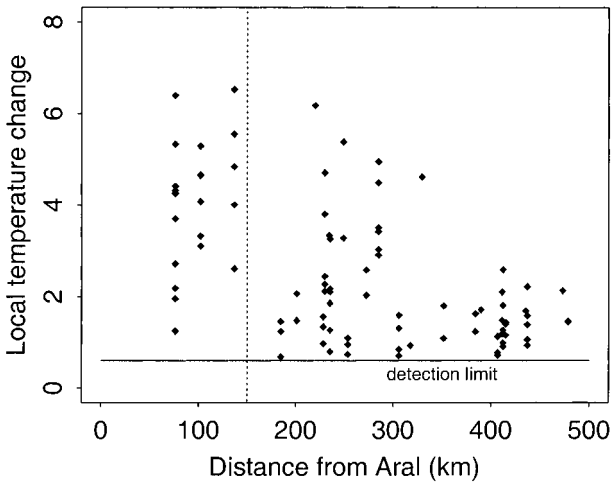

FIG. 8. Absolute values of mean temperature change (°C) from the local records plotted vs distance from the center of the Aral Sea (45°N, 60°E). Only changes that are significant above the 95% confidence level are shown, which represents 19% of all station–month combinations within the analysis region (Table 1). Points represent changes from all months. Each cluster of points at a particular distance shows the changes at a single station for all months. The 1960 Aral shoreline is 100–150 km from the center of the sea (dashed line). The solid horizontal line shows the detection limit for changes significant at the 95% confidence level.

decreases as the sea becomes shallower and its surface area is reduced, leading to a warming (cooling) in the spring–summer (autumn–winter).

The cooling observed along the northern edge of the sea during July (Fig. 7c) is inconsistent with the simple model of a weakened lake effect. Results from coupled regional atmospheric–lake model simulations show that this cooling is expected to accompany desiccation, as a result of interactions between the large-scale wind, a thermally driven mesoscale circulation, and the radiative effects of clouds (Small et al. 2001). Therefore, the warming–cooling pattern identified in July provides further evidence that the local temperature changes identified here are linked to Aral desiccation.

b. Temperature extremes

The local changes in maximum and minimum temperature are similar to the local changes in mean temperature. First, there are more significant changes in the local extreme time series than in the observed records (Table 1). Second, the magnitude of local extreme temperature changes is greatest near the sea and diminishes with distance from the shoreline. And third, the sign of local extreme temperature changes varies with season as expected to accompany desiccation (Fig. 10). One difference exists between the changes in the mean and daily extremes. During the months when mean temperature has locally warmed (e.g., July), the changes in maximum temperature are ~40% greater than the changes in mean temperature (Table 2). However, the changes in minimum temperature are roughly equal to the changes in mean temperature (Table 2). The reverse is true during months when a local cooling of mean temperatures exists—the local changes in minimum

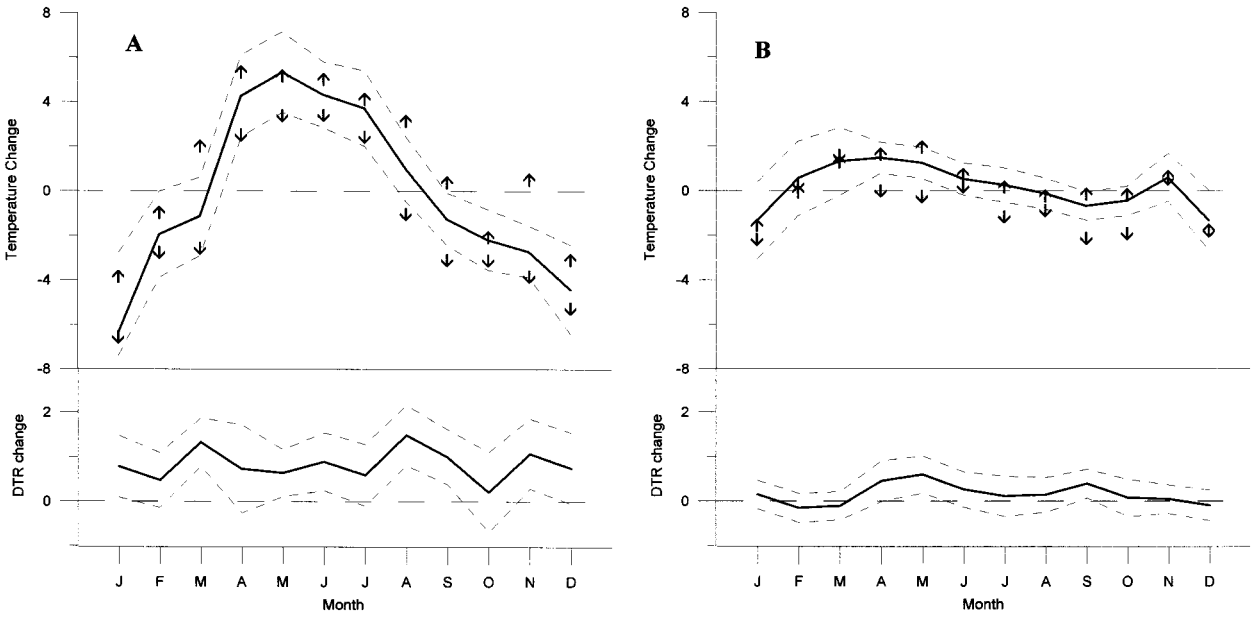

FIG. 9. Annual cycle of local temperature changes from two stations in the analysis region: (a) Barsakelmes Island [(BI) in Fig. 2]; and (b) a station which is 150 km east of the 1960 shoreline. The top plots show changes in mean temperature (thick line) and the 95% confidence interval estimates on these changes (gray dashed lines). The arrows show the changes in maximum (up arrow) and minimum temperature (down arrow). The bottom plot shows the changes in diurnal temperature range (thick line) and the 95% confidence interval estimates on these changes (gray dashed lines).

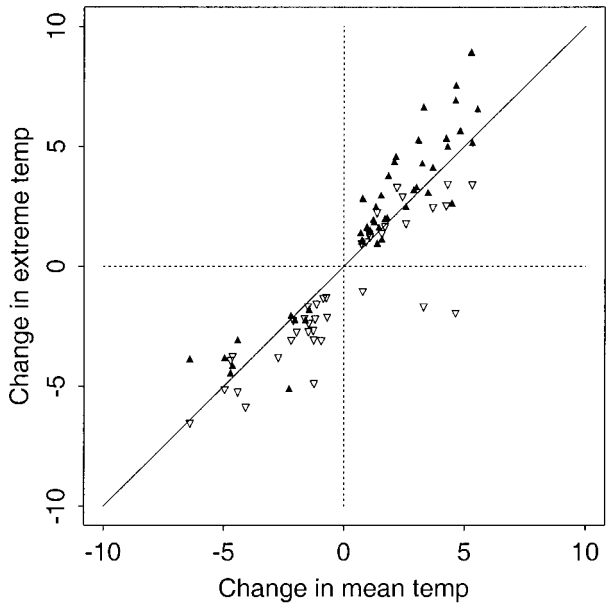

FIG. 10. Local changes in maximum (solid up triangle) and minimum (open down triangle) temperature as compared with local changes in mean temperature for each station within the analysis region. Only station–month combinations with extreme and mean temperature changes that are both significant above the 95% confidence level are plotted. The solid line shows the 1:1 line. Points falling above (below) the 1:1 line on the right (left) side of the plot show extreme changes that are greater in magnitude than mean changes.

temperature are enhanced by ~40% (i.e., a greater cooling) whereas the local changes in maximum temperature are roughly equal to the local changes in the mean. This enhancement of changes in either the maximum or minimum temperature is shown by plotting the changes in extremes against the changes in mean temperature (Fig. 10). Nearly all of the significant changes in maximum (minimum) temperature fall above (below) the 1:1 line when the mean temperature is increasing (decreasing).

c. DTR

Since 1960, there has been a local increase in the DTR in all months near the Aral because of the asymmetric local changes in the maximum and minimum temperatures—nearly all (~85%) of the significant DTR changes in the analysis region are positive. During spring and summer, the DTR has locally increased because maximum temperatures have increased more (by ~40%) than minimum temperatures (Table 2). The opposite occurs during autumn and winter (Table 2). The median increase in DTR throughout the entire analysis region is nearly 3°C, regardless of whether mean temperatures have increased or decreased (Table 2). As was the case for the changes in mean temperature, the increase in DTR is greatest near the Aral shoreline and diminishes with distance from the sea.

TABLE 3. Comparison of regional and local changes in air temperature for all stations within the analysis region: the percentage of occurrences when regional warming/cooling either enhances or offsets local warming/cooling, for stations with local changes that are significant above the 95% confidence level only. The boldface numbers show the most common category for each temperature variable.

	Regional warming enhances local warming	Regional warming offsets local cooling	Regional cooling offsets local warming	Regional cooling enhances local cooling
Mean	**37**	**37**	20	5
Max	**56**	28	25	0
Min	25	**61**	6	8
DTR	20	3	**67**	10

d. Comparison of local and regional changes

We have divided the observed climatic changes around the Aral Sea into local [$L(t)$] and regional [$R_T(t)$] components. We now compare the magnitude and sign of the local and regional changes to assess the contribution each part makes to the total observed changes. In most months, regional mean temperature has increased across the analysis region—warming is observed at 75% of all combinations of stations and months (Table 3). This increase in regional mean temperature is consistent with results from previous studies (e.g., Hurrell and van Loon 1997). For mean temperature, regional warming has enhanced local warming during spring–summer and offset local cooling during fall–winter. Regional mean temperatures have decreased during spring (25% of combinations; Table 3), which has offset the local warming that predominates during this season.

The regional changes in mean temperature are typically 45%–75% as large as local changes (median value;

TABLE 2. First two columns show the median ratio of local changes in extreme temperature to local changes in mean temperature and the sample size (n), for situations when the local mean temperature is increasing (first row) and decreasing (second row). The ratio was calculated at each station where the changes in both the extreme and mean were significant at the 95% level or above. The 95% confidence interval estimate of the median ratio is shown. The final column shows the median change in DTR (°C) and the sample size for cases when the mean is increasing and decreasing. The 95% contour interval estimate of the median DTR change is also shown. Only stations where DTR changes are significant at 95% confidence level are included.

Change in mean	Max Δ/Mean Δ	Min Δ/Mean Δ	Change in DTR (°C)
Warmer	1.41 ± 0.15 (n = 36)	1.01 ± 0.24 (n = 14)	2.78 ± 0.96 (n = 43)
Cooler	0.94 ± 0.14 (n = 10)	1.42 ± 0.12 (n = 24)	2.72 ± 0.47 (n = 50)

TABLE 4. The median value in the analysis region of the ratio of the regional change to the local change at each station. The median value is reported for three different minimum confidence levels. The dependence on confidence level exists because smaller local changes can be detected when the minimum confidence level, and therefore the detection limit, is lowered.

	Median of regional/local change Minimum confidence level		
	95%	90%	75%
Mean	0.43	0.53	0.75
Max	0.41	0.48	0.71
Min	0.59	0.61	0.68
DTR	0.18	0.18	0.21

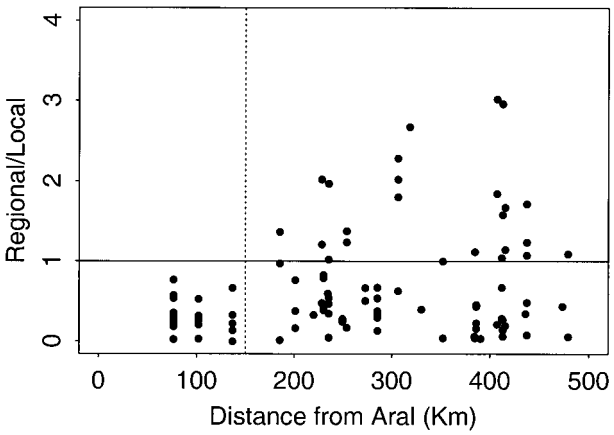

FIG. 11. Ratio of regional mean temperature changes to local mean temperature changes vs distance from the center of the Aral Sea for each station within the analysis region. Values < 1.0 (solid line) show local changes that are greater than regional changes. The 1960 Aral shoreline is 100–150 km from the center of the sea (dashed line). Only station–month combinations with local mean temperature changes that are above the 95% confidence level are plotted. If a lower confidence level was used (e.g., 90%), additional data points with higher ratios would exist. The dependence on confidence level exists because smaller local changes can be detected when the minimum confidence level, and therefore the detection limit, is lowered.

Table 4). The stations closest to the sea have recorded local changes that are several times greater than the corresponding regional value (Fig. 11). However, the regional changes are often equal or greater in magnitude than local changes more than ~250 km from the center of the sea, or ~100 km from the Aral shoreline. This shows that it is important to remove regional trends from observed records in order to define the spatial extent of the climatic changes driven by desiccation or other land surface modifications.

Typically, the regional maximum and minimum temperatures throughout the analysis region have also become warmer (Table 3). The primary effect is to enhance the local warming of maximum temperatures during spring–summer (56% of cases) and offset the local cooling of minimum temperatures during autumn–winter (61% of cases; Table 3). Again, the regional changes are typically 50%–75% as large as the local changes (Table 4) and the relative magnitude of the regional changes increases with distance from the sea.

Since 1960, the regional DTR has primarily decreased throughout the analysis region (Table 3). This change is consistent with previous studies that have shown DTR has decreased across much of the Northern Hemisphere (e.g., Karl et al. 1991). The local changes in DTR are nearly all positive. Therefore, the regionally consistent decrease in DTR has primarily offset local increases in DTR (Table 3). The regional DTR decreases, however, are typically only 20% as large as the local increases (Table 4). Again, the relative magnitude of regional changes increases with distance from the Aral.

e. Sensitivity to size of the analysis region

In section 3, we defined two assumptions critical to this analysis. The assumption that climatic variability and trends are spatially continuous at the length scale of the analysis region is supported by the substantial reduction of variance in the local temperature records when regional anomalies are removed (section 3e). We have not yet tested the second assumption that climatic changes driven by desiccation do not extend beyond the boundary of the analysis region. The result that few significant climatic changes exist near the boundary of the analysis region (e.g., Fig. 7) is not proof that this assumption is valid. If the local change were limited to the analysis region, we would expect few or no changes near the boundary. However, the lack of changes near the boundary may also indicate that the effects of desiccation extend beyond the boundary of the analysis region and that these changes have been incorporated into the regional signal.

In order to test the assumption that the local climatic changes do not extend beyond the 500-km radius analysis region used here, we repeated the entire analysis for July mean temperature for analysis regions with radii varying from 150 to 650 km in 50-km increments. July was chosen because the spatial extent and magnitude of the Aral Sea lake effect is substantial during this month (Small et al. 2001).

To quantify the effects of analysis region size, we compare the local warming recorded by a station in the largest analysis region (650 km) with the local warming recorded by the same station in each of the smaller analysis regions. This comparison yields a series of temperature differences (smaller region − largest region) for each station that we plot against the radius of the smaller region (Fig. 12). As expected, the local warming observed at a station is less for smaller analysis regions than for larger ones. When the analysis region is relatively small, the local warming extends beyond the boundary of the analysis region and is incorporated into the regional signal, $R_T(t)$. The regional temperature anomalies that include some fraction of the local warming are then subtracted from the observed record. The net result is a local signal that is an underestimate of

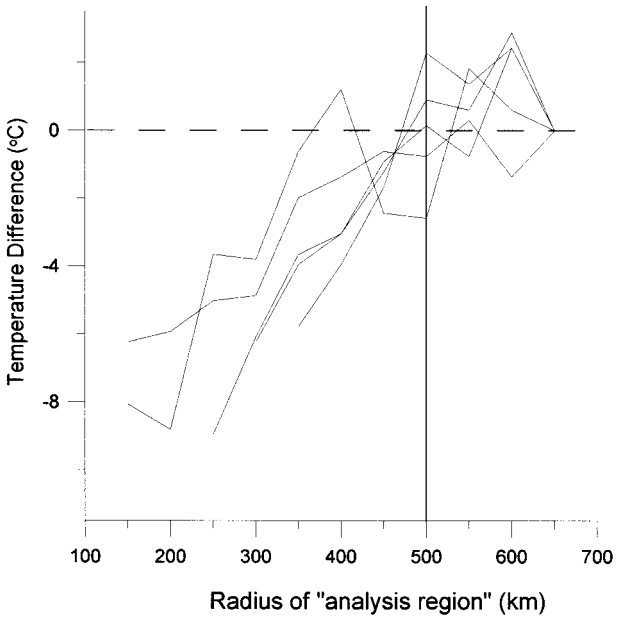

FIG. 12. Temperature difference between 1) the local change for an analysis region with radius shown by position on the *x* axis and 2) the local change for the largest analysis region (650 km). Results are for Jul mean temperature. Each line represents a station. If a station is $>$ 150 km from the center of the sea, the temperature difference cannot be calculated for the smallest analysis regions (i.e., some lines begin at $>$150 km on *x* axis). Results from only six stations are shown as others are similar. The vertical line at 500 km shows the radius of the analyzed region used in this study.

the true local change. Our results show that the local warming increases until the radius of the masked region is equal to 450 or 500 km (Fig. 12). For ''analysis regions'' $>$ $\sim$450 km in radius, the local changes are similar to the changes detected when the largest region (650 km) is used. Based on this analysis, we conclude that most or all of the local climatic changes caused by desiccation have occurred within 500 km from the center of the sea. This result is corroborated by model experiments (Small et al. 2001). Therefore, the assumption that the local changes are restricted to the analysis region (500 km) appears to be valid.

5. Discussion

a. Climatic changes caused by desiccation of the Aral Sea

As compared with the surrounding region, air temperature around the Aral Sea has changed substantially since 1960. Is desiccation of the Aral Sea the cause of these ''local'' temperature changes? Several features of the local climatic change identified here suggest this is the case. First, the spatial pattern of temperature changes pinpoints the source of the changes to be in the vicinity of the Aral Sea. The most significant and largest changes are along the 1960 Aral shoreline. The significance and magnitude of changes diminishes with increasing distance from the shoreline, with the most gradual reduction in changes occurring in the downwind direction. Second, the seasonal variations of the local temperature trends are consistent with the change to a shallower, less extensive lake. The most pronounced warming (cooling) occurs during the months when the lake–land temperature contrast would have been most negative (positive). Last, the changes in temperature extremes and DTR are consistent with a reduction in the magnitude of the sea's influence on the diurnal cycle. Coupled atmospheric-lake model experiments demonstrate that the observed changes in air temperature are driven by a reduction of the Aral Sea's thermal capacity where it has become shallower and by a reduction in thermal capacity and evaporation where the Aral has been replaced by desert (Small et al. 2001).

b. Data quality issues

Our results rely upon ''good data.'' However, the data used here (GSDD) have two major problems. First, there is limited documentation regarding station moves, changes in observation method, and other sources of inhomogeneities. Second, the records are not continuous. Higher-quality data would certainly allow for more accurate results. However, the spatially limited nature of desiccation limits the availability of numerous, high-quality records. This same problem hinders studies of other land surface modifications (e.g., Barnston and Schickedanz 1984), especially in areas of the world similar to central Asia.

The data used here are imperfect. However, several features of our results suggest that data quality issues have not substantially compromised this analysis. First, correcting for discontinuous records, for example by using the first difference method (Peterson et al. 1998), yields nearly identical results. Second, various sources of inhomogeneities (e.g., station moves) introduce random errors into climate records (Karl and Williams 1987). These errors should affect the records from stations in the analysis region differently, so they are not a reasonable source of the spatially consistent changes found here. Third, changes in observing practices could introduce trends that are consistent across some area. However, it seems unlikely that variations in observing practice would yield strong trends that are of opposite sign in summer and winter, minimal trends in spring and autumn (Fig. 9), and trends that are concentrated on the downwind side of the sea. In addition, many of the stations within and outside of the analysis region are in the same political units and would likely undergo similar changes in observing practice. The method used here would remove any trends that are common to both the analysis region and the surrounding areas. And fourth, the results from this statistical method are consistent with those from a physically based model (Small et al. 2001).

c. Climatic changes from other local perturbations

The method used here identifies climatic changes that are spatially restricted to some area. However, it does not isolate changes that are caused by a single forcing, such as desiccation. Therefore, it is possible that a spatially restricted forcing unrelated to desiccation may be the cause of part or all of the identified local changes. Previous studies have demonstrated that irrigation and urbanization result in temperature changes throughout the modified region (Barnston and Schickedanz 1984; Karl et al. 1988). Are either of these two modifications the source of the local climatic changes observed around the Aral Sea? For this to be the case, the climatic effects of irrigation or urbanization must be different within and outside of the analysis region.

Irrigation in semiarid areas like central Asia may decrease maximum temperatures by up to ~2°C, have little effect on minimum temperatures, and decrease the DTR by two degrees (e.g., Barnston and Schickedanz 1984). These temperature effects are mostly limited to the irrigated area and to the irrigation season that extends from mid-April to August in the Aral Sea region. There was a substantial increase in irrigation in the Aral Sea drainage basin after 1960. This irrigation indirectly caused Aral desiccation, as the water for the extensive irrigation projects was taken from the Amu and Syr Darya Rivers that flow into the Aral. Because most of the land irrigated since 1960 is greater than 500 km away from the Aral shoreline this irrigation likely had a negligible effect on air temperature around the sea. Near the Aral Sea, some new areas have been irrigated while some previously irrigated areas have been abandoned due to salinization and decreasing groundwater levels (Smith 1994). Therefore, we expect the effects of irrigation to be mixed in the Aral region since 1960. Importantly, the expected magnitude of temperature changes (either positive or negative) driven by variations in irrigation extent are small (1°–2°C) in comparison with the local changes observed here. In addition, irrigation effects are limited to the several-month-long irrigation season, whereas local changes in the Aral region are observed throughout the year. Overall, irrigation is probably not an important source of the local temperature changes that have occurred in the Aral Sea region since 1960.

Karl et al. (1988) and others have demonstrated that urbanization influences local air temperature. When compared with nearby rural environments, urban areas experience warmer minimum and mean temperatures, slightly cooler maximum temperatures, and therefore a decrease in diurnal temperature range. These temperature effects exist in all seasons, with the exception of the decrease in maximum temperature during the winter. The population of nearly all of the cities in the analysis region is $\sim 10^5$ or less. For cities of this size, the expected temperature changes from urbanization are less than 1°C (Karl et al. 1988). The urban temperature effects are likely small (<2°C) even for Nukus, which has the largest population ($\sim 5 \times 10^5$) on the Amu Darya Delta. The entire temperature changes caused by urbanization (~1°–2°C) have not occurred since 1960, since most of the cities in this region are centuries old. In addition, the population in some cities has remained constant or decreased since 1960 due to the environmental degradation in this region. Therefore, the temperature changes due to urbanization since 1960 are likely small (<1°C) in comparison with the local temperature changes we have identified here.

Changes in the hydrologic state of the Amu and Syr Darya Deltas, related to Aral Sea desiccation, are yet another source of local changes within the analysis region. The groundwater table in the Amu and Syr Darya Deltas has dropped substantially since 1960, leading to desiccation of wetlands and soils throughout the delta regions (Dukhovnyi et al. 1984; Sattarov et al. 1991; Smith 1994). Desiccation of wetlands and soils should yield temperature changes similar to those resulting from Aral Sea desiccation, although smaller in magnitude and spatial extent. The effects of delta and Aral desiccation should be cumulative in the Amu Darya Delta, because the prevailing surface winds have a northerly component during most months (Fig. 7). Therefore, it is not possible to separate the effects of these two different forcings.

6. Conclusions

1) Regionally coherent temperature trends, unrelated to desiccation of the Aral Sea, are observed across central Asia between 1960 and 1997. On a regional scale, mean, maximum, and minimum temperature have increased by ~1°–1.5°C in most months, whereas DTR has typically decreased. These regionally coherent trends are often more than half the magnitude of the local changes from Aral Sea desiccation. Therefore, they must be removed in order to establish quantitative estimates of the local climatic changes caused by desiccation. The method described and used here accomplishes this goal.
2) There is substantial year-to-year temperature variability that is coherent across central Asia. By using temperature observations from beyond the area that is influenced by desiccation, we have removed ~80%–90% of this variability in the temperature records from the Aral Sea region. Removing this variability substantially lowers the climate change detection limit, to 1°–2°C for most stations. This allows for a more exact estimate of the magnitude and spatial extent of local climatic changes.
3) The changes in mean and extreme air temperature unique to the Aral Sea region are very large, ranging from >2°C (the minimum detectable change) to 6°C, over a 38-yr interval. Several features of this local change indicate desiccation of the Aral Sea is the cause. First, the magnitude of local changes is great-

est along the 1960 shoreline and decreases with distance from the sea. Therefore, the most statistically significant changes are clustered near the sea. Second, warming (cooling) is observed during spring and summer (autumn and winter) as expected to accompany a weakening of the ''lake effect.'' Third, changes extend farthest in the downwind direction, up to ~200 km from the 1960 shoreline.

4) A local increase in DTR of 2°–3°C is observed near the Aral Sea in all months. This demonstrates a weakening of the lake's damping of the diurnal temperature cycle. The increase in DTR is the product of asymmetric changes in extreme temperature—maximum temperatures have increased more than minimum temperatures in months when desiccation has resulted in warming and vice versa.

Acknowledgments. This research was supported by NSF ATM-9632304. We thank Tim Hoar, Roseanna Neuppauer, Gordon Frioso, and Carrie Morrill for their assistance. Two anonymous reviewers provided very helpful reviews.

REFERENCES

Alpert, P., and M. Mandel, 1986: Wind variability—An indicator for a mesoclimatic change in Israel. *J. Climate Appl. Meteor.,* **25,** 1568–1576.

Barnston, A. G., and P. T. Schickedanz, 1984: The effect of irrigation on warm season precipitation in the southern Great Plains. *J. Climate Appl. Meteor.,* **23,** 865–888.

Bates, G. T., S. W. Hostetler, and F. Giorgi, 1995: Two-year simulation of the Great Lakes region with a coupled modeling system. *Mon. Wea. Rev.,***123,** 1505–1522.

Ben Gai, T., A. Bitan, A. Manes, and P. Alpert, 1993: Long-term change in October rainfall patterns in southern Israel. *Theor. Appl. Meteor.,* **46,** 209–217.

Changnon, S. A., and D. M. A. Jones, 1972: Review of the influences of the Great Lakes on weather. *Water Resour. Res.,* **8,** 360–371.

Chase, T. N., R. A. Pielke, T. G. F. Kittel, J. S. Baron, and T. J. Stohlgren, 1999: Potential impacts on Colorado Rocky Mountain weather due to land use changes on the adjacent Great Plains. *J. Geophys. Res.,* **104,** 16 673–16 690.

Dukhovnyi, V. A., R. M. Razakov, I. B. Ruziev, and K. A. Kosnazarov, 1984: The Aral Sea problem and environmental protection programs. *Probl. Osvoeniya Pustyn.,* **6,** 3–15.

Fowler, W. B., and J. D. Helvey, 1974: Effect of large-scale irrigation on climate in the Columbia Basin. *Science,* **184,** 121–127.

Gornitz, V., 1985: A survey of anthropogenic vegetation changes in West Africa during the last century. *Climatic Change,* **7,** 285–325.

Hostetler, S. W., F. Giorgi, G. T. Bates, and P. J. Bartlein, 1994: Lake–atmosphere feedbacks associated with paleolakes Bonneville and Lahontan. *Science,* **263,** 665–668.

Hurrell, J. W., and H. van Loon, 1997: Decadal variations in climate associated with the North Atlantic Oscillation. *Climatic Change,* **36,** 301–326.

Karl, T. R., and C. N. Williams, 1987: An approach to adjusting climatological time series for discontinuous inhomogeneities. *J. Climate Appl. Meteor.,* **26,** 1744–1763.

——, H. F. Diaz, and G. Kukla, 1988: Urbanization: Its detection and effect in the United States climate record. *J. Climate,* **1,** 1099–1123.

——, G. Kukla, V. N. Razuvayev, and M. J. Changery, 1991: Global warming—evidence for asymmetric diurnal temperature change. *Geophys. Res. Lett.,* **18,** 2253–2256.

Lofgren, B. M., 1997: Simulated effects of idealized Laurentian Great Lakes on regional and large-scale climate. *J. Climate,* **10,** 2847–2858.

Lowry, W. P., 1977: Empirical estimation of urban effects on climate: A problem analysis. *J. Appl. Meteor.,* **16,** 129–135.

Lydolph, P. E., 1977: *Climates of the Soviet Union.* Elsevier Scientific Publishers, 443 pp.

Micklin, P. P., 1988: Desiccation of the Aral Sea: A water management disaster in the Soviet Union. *Science,* **241,** 1170–1176.

Miner, T. J., and J. M. Fritsch, 1997: Lake-effect rain events. *Mon. Wea. Rev.,* **125,** 3231–3248.

Myers, N., 1991: Tropical forests: Present status and future outlook. *Climatic Change,* **19,** 3–32.

Nychka, D., and N. Saltzmann, 1998: Design of air quality monitoring networks. *Case Studies in Environmental Statistics.* D. Nychka, L. Cox, and W. Piegorsh, Eds., Springer-Verlag, 3–15.

Otterman, A. M., S. Rubin, P. Alpert, and D. O'C. Starr, 1990: An increase of early rains in southern Israel following land-use change? *Bound.-Layer Meteor.,* **53,** 333–351.

Peterson, T. C., T. R. Karl, P. F. Jamason, R. Knight, and D. R. Easterling, 1998: First difference method: Maximizing station density for the calculation of long-term global temperature change. *J. Geophys. Res.,* **103,** 25 967–25 974.

Sattarov, D. S., V. E. Sektimenko, and V. G. Popov, 1991: State of soil cover in the Aral region in conjunction with the drying of the Aral Sea. *Pochvovedniye,* **23,** 5–9.

Schneider, S. H., 1994: Detecting climatic change signals: Are there any ''fingerprints''? *Science,* **263,** 341–347.

Shuttleworth, W. J., 1991: The Modellion concept. *Rev. Geophys.,* **29,** 585–606.

Sloan, L. C., 1994: ''Equable'' climates during the early Eocene. Significance of regional paleogeography for North American climate. *Geology,* **22,** 881–884.

Small, E. E., F. Giorgi, and L. C. Sloan, 1999: Regional climate model simulation of precipitation in central Asia: Mean and interannual variability. *J. Geophys. Res.,* **104,** 6563–6582.

——, ——, ——, and S. Hostetler, 2001: The effects of desiccation and climatic change on the hydrology of the Aral Sea. *J. Climate,* **14,** 300–322.

Smith, D. R., 1994: Change and variability in climate and ecosystem decline in Aral Sea basin deltas. *Post-Sov. Geogr.,* **35,** 142–165.

Steinberger, E. H., and N. Gazit-Yaari, 1996: Recent changes in the spatial distribution of annual precipitation in Israel. *J. Climate,* **9,** 3328–3336.

Zheng, X., E. B. Reid, and C. S. Thompson, 1997: Trend detection in regional-mean temperature series. Maximum, minimum, mean, diurnal range, and SST. *J. Climate,* **10,** 317–326.